Theoretical study of molecular electronic excitations and optical transitions of C_{60}

A. V. Nikolaev,* I. V. Bodrenko, and E. V. Tkalya†
Algodign LLC, Bolshaya Sadovaya 8/1, Moscow 123001, Russia
(Received 13 June 2007; published 7 January 2008)

We report results of *ab initio* calculations of excited states of the fullerene molecule using the configuration-interaction approach with singly excited determinants (SCI). We have used both experimental geometry and the geometry optimized by the density functional method and worked with basis sets at the correlation-consistent polarization valence triple-ζ (cc-pVTZ) and augmented cc-pVTZ levels. In contrast to the early SCI semiempirical calculations, we find that the two lowest $^1T_{1u} \leftarrow {}^1A_g$ electron optical lines are situated at relatively high energies of ~5.8 eV (214 nm) and ~6.3 eV (197 nm). These two lines originate from two $^1T_{1u} \leftarrow {}^1A_g$ transitions: from the highest occupied molecular orbital (HOMO) to one above the lowest unoccupied molecular orbital (LUMO+1) ($6h_u \rightarrow 3t_{1g}$) and from (HOMO−1) to LUMO ($10h_g \rightarrow 7t_{1u}$). The lowest molecular excitation, which is the $1\ ^3T_{2g}$ level, is found at ~2.5 eV. Inclusion of doubly excited determinants leads only to minor corrections to this picture. We discuss possible assignment of absorption bands at energies smaller than 5.8 eV (or λ larger than 214 nm).

DOI: 10.1103/PhysRevA.77.012503 PACS number(s): 31.15.V−, 36.20.Kd, 81.05.Tp

I. INTRODUCTION

The buckminsterfullerene molecule C_{60} has attracted much attention from theoreticians since its discovery in 1985 [1,2]. Indeed, the role of the fullerene molecule in quantum chemistry is unique because its highest molecular symmetry group (I_h) leads to a high degeneracy of molecular orbitals (MOs). The MOs of C_{60} are classified according to irreducible representations (irreps) of I_h, which are a, t_1, t_2, g, and h. (The dimensions of the irreps are one, three, three, four, and five, respectively.) For example, the highest occupied molecular orbital (HOMO) is a fivefold electron shell of h_u symmetry, while the lowest unoccupied molecular orbital (LUMO) is a threefold level of t_{1u} symmetry.

High degeneracies of molecular orbitals imply a complex electronic structure [3–6]. However, since all electron shells of the neutral C_{60} molecule are completely filled, the ground state is of ^1A_g symmetry and the many-electron states of the molecule are not revealed. The situation changes when the fullerene molecule is excited. Then a few electrons of C_{60} are promoted to a higher energy, and some of the electron shells become open. The electrons of the open shells exhibit correlated behavior and form many-electron levels called molecular terms [2,7–10], which are also classified according to the irreducible representations of the icosahedral symmetry (A, T_1, T_2, G, and H). Thus, a careful study of these correlations is needed for calculations of optical transitions [12,13] and molecular excitations. Because of the unique high molecular symmetry involved, the Jahn-Teller effect plays an important role and strongly influences the fullerene properties [14]. It is worth mentioning that intramolecular correlations and the Jahn-Teller effect are vital for understanding the physics of alkali-metal-doped fullerites, which exhibit superconductivity, magnetic behavior, and metal-insulator transitions [2,14–16]. In the present study we will also show that the strong electron-vibronic coupling is possibly responsible for the two lowest optical bands of the fullerene molecule.

Computation of the many-electron states of C_{60} is a challenge for the modern quantum theory [17]. In the literature there are few works devoted to the problem of calculations of molecular excitations of fullerene [7–11]. Nearly all of them are semiempirical and are based only on singly excited configuration interaction (CI). We reproduce some of their computed levels in Table I. In Ref. [11] the authors investigated the optical response of C_{60} computed from single-particle wave functions determined from density functional theory (DFT) with the local density approximation. The calculation of Negri *et al.* [8] employed a semiempirical quantum consistent force field method for π-electrons (QCFF/π), and took into account 196 configuration state functions (CSFs). The first excited state ($1\ ^3T_{2g}$) was found at 2.06 eV, and the $1\ ^1T_{1u}$ and $2\ ^1T_{1u}$ levels at 4.08 and 4.53 eV. A Pariser-Parr-Pople configuration interaction (PPPCI) calculation that includes 134 CSFs finds the first three $^1T_{1u}$ levels at 4.00, 4.68, and 6.69 eV, with the first excited $^3T_{2g}$ level at 2.23 eV. Finally, complete neglect of differential overlap for spectroscopy (CNDO/S) calculations of Braga *et al.* based on 808 and 900 configurations predict that $1\ ^1T_{1u}$ is lowered to 3.4 eV, while the three most intense transitions are at 4.38, 5.24, and 5.78 eV. Unfortunately, all of the CI calculations reported in Refs. [7–10] are crucially dependent on a number of approximations for matrix elements and therefore cannot be considered as true *ab initio* approaches. The calculations of Westin *et al.* [11], although they go beyond simple Hartree-Fock treatment of the optical spectrum, are not based on the concept of configuration interaction. In addition to the well-known shortcomings of the local density approximation for ground-state wave functions, numerical results depend on the effective screening parameter ν.

In the present study, in comparison with Refs. [7–11], we employ the *ab initio* treatment without effective parameters,

*Also at Institute of Physical Chemistry of RAS, Leninskii prospekt 31, 117915, Moscow, Russia; Alexander.Nikolaev@Algodign.com
†Also at Institute of Nuclear Physics, Moscow State University, 119992 Moscow, Vorob'evy Gory, Russia.

TABLE I. Selected molecular excitations calculated with semiempirical CI calculations and in the present work. Energies are in eV. N_{CSF} stands for the number of configuration state functions used for CI calculation.

Reference	[9]		[8]	[10]	This work
Method	PPP		QCFF/π	CNDO/S	*Ab initio* SCI
N_{CSF}	134		266	900	2857
	Planar	3D			
$1\ ^3T_{2g}$	2.456	2.232	2.06		2.549
$1\ ^1G_u$	3.603	3.381	3.21		4.700
$1\ ^1H_u$	3.635	3.391	3.15		4.771
$1\ ^1T_{1u}$	4.227	4.000	4.08	3.40	5.796
$2\ ^1T_{1u}$	4.750	4.681	4.53	4.06	6.335

which represents a new level of CI calculation of the fullerene molecule.

II. METHOD OF CALCULATION

A. Configuration interaction

A well-known recipe for correlations is the method of configuration interaction [17]. The basic idea is to diagonalize the N-electron Hamiltonian in a basis of N-electron functions (Slater determinants). In principle, the full CI method with infinite number of molecular orbitals provides an exact solution of the many-electron problem. In practice, even for small molecules and moderately sized one-electron basis sets, the number of N-electron determinants is enormous. To avoid it, we first introduce an active space which comprises a set of highest occupied molecular orbitals (HOMOs) and a set of lowest unoccupied molecular orbitals (LUMOs). The space of the MOs is divided into three subspaces: the inactive, the active, and the external orbitals. The inactive orbitals are doubly occupied, while the external orbitals are unoccupied. Within the chosen active space one can consider various approximations to the complete active space CI matrix by truncating the many-electron trial function at some excitation level. For example, the singly excited CI (SCI) approach has been proven to be adequate as a first approximation for the neutral molecule because all electron shells of C_{60} are filled up. In the following, for large active spaces (ASs), we use SCI, but also consider singly and doubly excited determinants (SDCI) for smaller ASs, and a complete active space (CAS) CI method [18] for important active spaces of two molecular shells (eight MOs). The computer code for the CI calculations is a modified and extended version of the earlier program, Ref. [5].

B. Computational details

The CI calculations have been carried out with the set of molecular orbitals (MOs) obtained from the restricted Hartree-Fock (RHF) self-consistent-field calculation [17] of the neutral fullerene molecule. In the following we have used two sets of coordinates of the C_{60} molecule. The first set was obtained in Ref. [19] (DFT method). The two different C-C bond lengths were $R_5=1.4507$ Å (C-C bond in pentagons) and $R_6=1.3906$ Å (short C-C bond in hexagons). The second set corresponds to the experimental geometry [20] with $R_5=1.448$ Å and $R_6=1.404$ Å.

We have used our original RHF computer program [21], which uses the resolution of the identity [22] (RI) method for calculation of the two-electron Coulomb integrals. The series of the RI (auxiliary) basis sets, HCNO.x, were designed for RI-convergent calculations of the RHF total energies and the electronic properties of molecules containing hydrogen, carbon, nitrogen, and oxygen elements as discussed in [21]. Here x indicates (but is not exactly equal to) the accuracy (in atomic units) of the total RHF energy per atom: a smaller x implies more RI functions and a more accurate RI basis set. The accuracy of the RI basis set is almost independent of the choice of molecular basis set. Having performed test calculations with Pople's 6-31G* MO basis set [23,24] and the HCNO.x RI series, we have found that a reasonable convergence is achieved for the HCNO.001 RI basis set, which is used for all further calculations.

Throughout the paper, we have adopted the shorthand notation aug-cc-pVTZ($-f$) for Dunning's augmented correlation-consistent polarizable valence triple-ζ molecular basis set (aug-cc-pVTZ) [24,25], where all polarization functions of f symmetry are excluded from the set.

III. RESULTS AND DISCUSSION

A. SCI excitation spectrum of C_{60}

The main results are shown in Tables II and III. The (HOMO−4) to (LUMO+18) energies of C_{60} calculated with the aug-cc-pVTZ($-f$) basis set are quoted in Table II. We then define a broad active space spanned by these MOs and occupied with 42 correlated electrons and use it in our SCI calculations. Table III displays the resulting spectrum of lowest molecular excitations. In order to evaluate the influence of the two bond lengths of the fullerene molecule, we have performed calculations with two different geometries of C_{60}: the one optimized by DFT [19] (optimized geometry (OG)) and the experimental geometry (EG) [20]. Inspection of Table III shows that the order of levels is mainly conserved, while a typical numerical deviation is ~0.2 eV. From this we conclude that a possible small change of the C_{60} bond lengths does not change appreciably its excitation spectrum.

The most striking feature of the calculation is the relatively high-energy position of the two lowest $^1T_{1u}$ excitations

TABLE II. Electron shells of C_{60}. E_{MO} is the one-electron Hartree-Fock MO energy (in eV). The basis set is aug-cc-pVTZ($-f$). $E_{tot}=-61\,832.163$ a.u.

	MOs	Symmetry	E_{MO}
LUMO+18	244–248	$8h_u$	4.303
LUMO+17	239–243	$14h_g$	3.855
LUMO+16	235–238	$8g_g$	3.794
LUMO+15	232–234	$10t_{2u}$	3.300
LUMO+14	229–231	$4t_{1g}$	3.280
LUMO+13	228	$6a_g$	3.161
LUMO+12	225–227	$8t_{1u}$	3.115
LUMO+11	220–224	$7h_u$	2.557
LUMO+10	215–219	$13h_g$	2.418
LUMO+9	211–214	$7g_g$	2.254
LUMO+8	206–210	$12h_g$	2.121
LUMO+7	203–205	$9t_{2u}$	1.994
LUMO+6	200–202	$8t_{2u}$	1.774
LUMO+5	196–199	$7g_u$	1.751
LUMO+4	195	$5a_g$	1.496
LUMO+3	190–194	$11h_g$	1.398
LUMO+2	187–189	$7t_{2u}$	1.150
LUMO+1	184–186	$3t_{1g}$	0.947
LUMO	181–183	$7t_{1u}$	−0.817
HOMO	176–180	$6h_u$	−7.834
HOMO−1	171–175	$10h_g$	−9.627
HOMO−2	167–170	$6g_u$	−9.890
HOMO−3	163–166	$6g_g$	−12.589
HOMO−4	160–162	$6t_{2u}$	−13.050

(given already in Table I) with oscillator strengths 1.02 and 0.16, respectively. For a review on oscillator strengths in semiempirical calculations, see Ref. [11]. In the following, we limit ourselves to the optimized geometry [19] and consider mainly the problem of convergency and adequacy of the SCI calculation, leaving discussion and conclusions until Sec. IV.

B. Molecular basis set dependence

To study the basis set dependence of the SCI excitation spectrum we narrowed the active space to 167–219 MOs; see Table II. This active space consists of 14 electron shells (from HOMO−2 to LUMO+10) filled by 28 correlated electrons. Such calculations require less computer time in comparison with the calculation with the active space of Table II reported in Table III, but lead to a less accurate molecular excitation spectrum.

The results of such SCI calculations are presented in Table IV. Notice that the order of the levels is almost the same for the group of 6-31G*, cc-pVDZ, cc-pVTZ, and cc-pVTZ($-f$) basis sets. The deviations of the molecular excitation energies are rather small, of the order of 0.1 eV. The molecular energies are close to a convergence and the basis f functions have a small effect on the calculated values. On the other hand, the inclusion of diffuse functions in aug-cc-pVDZ($-f$) and aug-cc-pVTZ($-f$) basis sets leads to a rearrangement of electronic levels, Table IV, which indicates that aug-cc-pVTZ($-f$) is the best set for SCI calculations.

C. Active space dependence

Here we study the dependence of SCI excitation energies on the choice of active space. In Table V we keep the lower-

TABLE III. Lowest excitations of C_{60}. OG refers to the bond lengths of C_{60} optimized by DFT, Ref. [19], EG to the experimental values, Ref. [20].

	$^3T_{2g}$	$^3T_{1g}$	$^1T_{2g}$	^3H_g	$^1T_{1g}$	^3G_g	^1G_g	^3G_u
OG	2.549	3.041	3.229	3.287	3.416	3.417	3.538	3.595
EG	2.384	2.877	3.051	3.100	3.239	3.235	3.357	3.464
	$^3T_{1u}$	$^3T_{2u}$	^1H_g	^3H_u	$^1T_{2u}$	^1G_u	^1H_u	$^3T_{2u}$
OG	3.917	3.996	4.079	4.304	4.611	4.700	4.771	4.960
EG	3.771	3.801	3.906	4.154	4.447	4.534	4.588	4.822
	^3G_u	^1G_u	^3G_g	^3H_u	^1H_u	^3H_u	$^1T_{1u}$	$^3T_{1u}$
OG	5.163	5.291	5.355	5.454	5.598	5.732	5.796	5.972
EG	5.023	5.157	5.300	5.295	5.445	5.662	5.667	5.849
	^3H_u	$^1T_{2u}$	^3G_u	$^3T_{2g}$	^1H_u	^1G_u	^3H_u	^1H_u
OG	5.986	6.001	6.019	6.124	6.141	6.208	6.236	6.264
EG	5.823	5.872	5.873	6.041	5.954	6.021	6.188	6.218
	$^1T_{1u}$	^3G_u	$^3T_{1u}$	^1H_g	$^3T_{2u}$	$^1T_{2g}$	^3H_u	^3H_g
OG	6.335	6.337	6.340	6.412	6.422	6.444	6.501	6.518
EG	6.182	6.216	6.206	6.340	6.275	6.360	6.395	6.400

TABLE IV. Energy spectrum of C_{60} with various basis sets. Basis sets are cc-pVDZ (DZ), aug-cc-pVDZ (aDZ), cc-pVTZ (TZ), cc-pVTZ without the f functions [TZ(−f)], and aug-cc-pVTZ(−f) [aTZ(−f)]; see text for details.

Γ	6-31G*	DZ	TZ	TZ(−f)	Γ	aDZ	Γ	aTZ(−f)
$^3T_{2g}$	2.593	2.575	2.582	2.573	$^3T_{2g}$	2.900	$^3T_{2g}$	2.669
$^3T_{1g}$	3.114	3.071	3.053	3.048	$^3T_{1g}$	3.261	$^3T_{1g}$	3.107
$^1T_{2g}$	3.322	3.276	3.249	3.248	$^1T_{2g}$	3.325	$^1T_{2g}$	3.254
^3H_g	3.384	3.336	3.312	3.308	^3H_g	3.474	^3H_g	3.390
$^1T_{1g}$	3.522	3.467	3.434	3.432	$^1T_{1g}$	3.541	$^1T_{1g}$	3.439
^3G_g	3.540	3.481	3.447	3.445	^3G_g	3.547	^3G_g	3.477
^1G_g	3.654	3.594	3.558	3.556	^1G_g	3.649	^1G_g	3.578
^3G_u	3.672	3.675	3.700	3.685	$^3T_{1u}$	4.154	^3G_u	3.995
$^3T_{1u}$	3.899	3.884	3.884	3.875	$^3T_{2u}$	4.196	$^3T_{1u}$	4.069
$^3T_{2u}$	4.002	3.993	3.995	3.987	^1H_g	4.288	$^3T_{2u}$	4.132
^1H_g	4.231	4.159	4.112	4.111	^3G_u	4.355	^1H_g	4.136
^3H_u	4.383	4.365	4.365	4.356	^3H_u	4.754	^3H_u	4.541
$^1T_{2u}$	4.650	4.632	4.625	4.618	$^1T_{2u}$	4.889	$^1T_{2u}$	4.751
^1G_u	4.831	4.802	4.779	4.777	^1G_u	4.897	^1G_u	4.849
^1H_u	4.862	4.835	4.816	4.811	^1H_u	4.976	^1H_u	4.899
$^3T_{2u}$	5.120	5.075	5.053	5.045	$^3T_{2u}$	5.500	$^3T_{2u}$	5.241
^3G_u	5.402	5.337	5.293	5.289	^3G_u	5.651	^3G_u	5.350
^3G_g	5.443	5.398	5.392	5.373	^1G_u	5.771	^1G_u	5.451
^1G_u	5.514	5.448	5.404	5.400	^3H_u	5.603	^3H_u	5.529
^3H_u	5.576	5.524	5.490	5.486	^1H_u	5.722	^1H_u	5.652
^1H_u	5.764	5.704	5.661	5.659	$^1T_{1u}$	6.116	$^1T_{1u}$	5.880
$^1T_{1u}$	5.873	5.826	5.793	5.785	^3H_u	6.221	^3G_g	5.919
^3H_u	5.940	5.859	5.810	5.797	$^1T_{2u}$	6.236	$^1T_{2u}$	6.071
$^3T_{1u}$	6.057	5.992	5.946	5.937	^3G_g	6.249	^3H_u	6.075
^3H_u	6.087	6.032	5.993	5.987	$^3T_{1u}$	6.280	$^3T_{1u}$	6.092
^3G_u	6.116	6.067	6.030	6.022	^1H_u	6.254	^3H_g	6.098
$^1T_{2u}$	6.165	6.096	6.048	6.046	^1G_u	6.281	^3G_u	6.103
$^3T_{2g}$	6.194	6.113	6.054	6.042	$^3T_{2g}$	6.543	^1H_u	6.198
^1H_u	6.299	6.246	6.202	6.199	$^1T_{1u}$	6.577	^1G_u	6.264
^1G_u	6.363	6.314	6.274	6.271	^3G_u	6.954	$^3T_{2g}$	6.325
^3G_u	6.445	6.386	6.346	6.340	^3H_g	6.960	$^1T_{1u}$	6.371
$^3T_{1u}$	6.457	6.402	6.360	6.356	$^3T_{1u}$	7.118	$^3T_{1u}$	6.413
$^1T_{1u}$	6.462	6.407	6.365	6.362	$^1T_{1u}$	7.122	^3G_u	6.452

boundary active shell, which is the HOMO−4 ($6t_{2u}$) level, unchanged and systematically increase the upper electron boundary. Inspection of Table V shows that we are close to a convergence for the broad active space of 160–248 MOs, shown in Table II. Therefore, we do not expect drastic changes if the active space is increased even further. Notice, however, that the optically active $1\ ^1T_{1u}$ and $2\ ^1T_{1u}$ levels monotonically decrease with the increase of the active space.

D. Beyond the SCI approximation for small AS

We recall that all the results reported earlier were obtained under the approximation that only singly excited configurations are taken into account. It is therefore instructive to estimate the accuracy of this assumption. Since the active space shown in Table II is very big, we study this problem by considering fewer active MOs. We limit ourselves to the four most important active spaces: HOMO+LUMO ($6h_u+7t_{1u}$), HOMO+(LUMO+1) ($6h_u+3t_{1g}$), (HOMO−1)+LUMO ($10h_g+7t_{1u}$), and (HOMO−1)+(LUMO+1) ($10h_g+3t_{1g}$). All of them consist of eight active MOs (five from h and three from t_1), which accommodate ten correlated electrons. For each of the active spaces we have performed four calculations: SCI, singly and doubly excited CI (SDCI), singly, doubly, and triply excited CI (SDTCI), and with all possible excitations. The latter is the so-called complete active space (CASCI) calculation [18]. In Tables VI–IX we give the results for the four cases, respectively. Notice that the CASCI results are very close to those of SDTCI, while both SCI and SDCI molecular energies miss the precise values by a typical

TABLE V. Dependence of selected energy levels on chosen active space. The active space consists of the MOs between the lower and upper MOs. The lower MO is 160, which corresponds to the HOMO−4 ($6t_{2u}$) level. The upper MO changes from LUMO+1 to LUMO+18. The basis set is aug-cc-pVTZ(−*f*).

Upper MO	186	189	194	199	202	205	210	214
$1\ ^3T_{2g}$	2.889	2.889	2.889	2.889	2.887	2.833	2.713	2.712
$1\ ^1G_u$	4.808	4.808	4.808	4.808	4.807	4.801	4.758	4.758
$1\ ^1H_u$	4.898	4.898	4.898	4.898	4.898	4.891	4.836	4.836
$1\ ^1T_{1u}$	6.230	6.230	6.230	6.230	6.230	6.212	6.028	6.026
$2\ ^1T_{1u}$	7.210	7.210	7.194	7.172	7.112	6.936	6.421	6.419
Upper MO	219	224	227	231	234	238	243	248
$1\ ^3T_{2g}$	2.633	2.633	2.623	2.618	2.600	2.599	2.584	2.549
$1\ ^1G_u$	4.730	4.730	4.727	4.721	4.719	4.719	4.715	4.700
$1\ ^1H_u$	4.802	4.802	4.798	4.793	4.791	4.790	4.785	4.771
$1\ ^1T_{1u}$	5.862	5.862	5.862	5.860	5.839	5.838	5.816	5.796
$2\ ^1T_{1u}$	6.354	6.354	6.352	6.352	6.348	6.348	6.343	6.335

error of ~0.1 eV. Furthermore, as a rule, SDCI energies overestimate the real values. It is very probable that the same conclusions are applicable to a calculation with a large AS. Indeed, our SDCI calculations [26] with a large AS of 186–248 MOs unambiguously indicate an increase of $^1T_{1u}$ energies in comparison with the SCI values: the energy of the first transition changes from 5.997 to 6.291 eV, and the energy of the second from 6.395 to 7.154 eV. Thus the SDCI results underline the importance of SDTCI calculations for the C_{60} molecule.

It is worth noting that the two lowest $^1T_{1u} \leftarrow {}^1A_g$ transitions can be found already in Tables VII and VIII. Their energies are quite high, 6.44 eV ($6h_u \rightarrow 3t_{1g}$) and 6.96 eV ($10h_g \rightarrow 7t_{1u}$). If both of the $^1T_{1g}$ levels are included in a CI calculation, they interact with each other, because they are of the same symmetry. Nevertheless, the lowest $1\ ^1T_{1u}$ level remains predominantly of $6h_u \rightarrow 3t_{1g}$ origin, while the $2\ ^1T_{1u}$ level is mainly of $10h_g \rightarrow 7t_{1u}$ character. Notice that the lowest part of the molecular excitations of C_{60} stems from the HOMO+LUMO ($6h_u+7t_{1u}$) active space, Table VI.

TABLE VI. Lowest excitations of C_{60}, calculated with ten correlated electrons in the $6h_u+7t_{1u}$ limited active space (see text for details).

Excitation level	S	SD	SDT	All (CAS)
^1A_g	0	0	0	0
$^3T_{2g}$	3.312	3.383	3.338	3.338
$^3T_{1g}$	3.482	3.551	3.511	3.511
$^1T_{2g}$	3.590	3.661	3.622	3.623
^3H_g	3.640	3.699	3.651	3.651
$^1T_{1g}$	3.691	3.761	3.713	3.713
^3G_g	3.709	3.768	3.726	3.726
^1G_g	3.769	3.833	3.791	3.791
^1H_g	4.298	4.337	4.281	4.280

IV. DISCUSSION AND CONCLUSIONS

We have found that the lowest electron optical transitions are at ~5.8 eV (214 nm) and ~6.3 eV (197 nm), which are in disagreement with the results obtained with the early semiempirical CI calculations [8–10]. We have analyzed the influence on the SCI excitation spectrum of the approximations used in our calculation and concluded that all of them are unlikely to change the computed values substantially. Thus, according to our calculations, the first allowed optical transition of C_{60} lies very close to the characteristic interstellar absorption at 217 nm [1,27].

From the *ab initio* study, we come to the conclusion that early semiempirical configuration interactions of the fullerene molecule, Refs. [8–10], result in systematically smaller excitation energies (see Table I). This was also the case for the molecular ion C_{60}^{2-}, for which the ^1A_g spin singlet ground state was obtained [28]. As shown in Refs. [5,6], the ground state is rather the $^3T_{1g}$ spin triplet in accordance with Hund's rules.

TABLE VII. Lowest excitations of C_{60}, calculated with ten correlated electrons in the $6h_u+3t_{1g}$ limited active space (see text for details).

Excitation level	S	SD	SDT	All (CAS)
^1A_g	0	0	0	0
$^3T_{2u}$	5.188	5.322	5.239	5.239
$^3T_{1u}$	5.234	5.368	5.297	5.298
^3G_u	5.410	5.544	5.470	5.471
^3H_u	5.461	5.595	5.529	5.530
^1H_u	5.550	5.684	5.616	5.617
^1G_u	5.594	5.728	5.661	5.662
$^1T_{2u}$	5.692	5.826	5.760	5.761
$^1T_{1u}$	6.443	6.577	6.438	6.439

TABLE VIII. Lowest excitations of C_{60}, calculated with ten correlated electrons in the $10h_g+7t_{1u}$ limited active space (see text for details).

Excitation level	S	SD	SDT	All (CAS)
^1A_g	0	0	0	0
^3G_u	5.218	5.497	5.331	5.334
$^3T_{1u}$	5.233	5.512	5.371	5.374
$^3T_{2u}$	5.440	5.719	5.562	5.565
^3H_u	5.457	5.737	5.596	5.600
$^1T_{2u}$	5.548	5.828	5.679	5.682
^1G_u	5.580	5.860	5.716	5.720
^1H_u	5.605	5.884	5.737	5.741
$^1T_{1u}$	6.997	7.277	6.959	6.960

The calculated oscillator strengths of the two lowest optical transitions to $1\ ^1T_{1u}$ and $2\ ^1T_{1u}$ states in the largest AS (Table II) are 1.02 and 0.16, respectively. The QCFF/π method employed by Negri *et al.* [8] resulted in 0.61 and 0.41 for the oscillator strengths of the two lowest transitions, while Braga *et al.* [10] (CNDO/S method) obtained 0.08 and 0.41. However, early semiempirical calculations give only a vague correspondence with the experimental optical density [12] (see Fig. 14 of Ref [11]). In order to achieve a good comparison, Westin *et al.* used a screened response oscillator strength distribution calculated with an adjustable parameter ν [11]. Under such conditions the theoretical curve reproduces the three experimental bands shown in Fig. 1. As we remarked before, our *ab initio* energies of the two lowest $^1T_{1u}$ transitions are very different from the semiempirical ones, and a direct comparison of the oscillator strengths is probably premature. The oscillator strengths in many cases show extreme sensitivity to the accuracy of the wave functions which hinders the comparison at the present stage. Our present *ab initio* study accounts only for the 6 eV band, Fig. 1, while the two other bands are probably of electron-vibronic origin [29]. The situation is not uncommon for complex molecules; it occurs, for example, at the $^1B_{2u}\leftarrow{}^1A_{1g}$ (3200 Å) transition of naphthalene as discussed in Chap. II.1γ of Ref. [29]. To illustrate the possibility of vibronically assisted bands, we simulate the density of singlet states by plotting broadened singlet lines in Fig. 1(b). It shows that the positions of the dipole-forbidden transitions are in the vicinity of the first two peaks.

TABLE IX. Lowest excitations of C_{60}, calculated with ten correlated electrons in the $10h_g+3t_{1g}$ limited active space (see text for details).

Excitation level	S	SD	SDT	All (CAS)
^1A_g	0	0	0	0
^3H_g	7.072	7.110	7.075	7.075
$^3T_{2g}$	7.116	7.154	7.125	7.125
^3G_g	7.174	7.224	7.194	7.194
$^3T_{1g}$	7.192	7.236	7.209	7.209
$^1T_{2g}$	7.299	7.348	7.320	7.320
$^1T_{1g}$	7.337	7.383	7.353	7.353
^1G_g	7.388	7.442	7.415	7.415
^1H_g	7.868	7.898	7.859	7.859

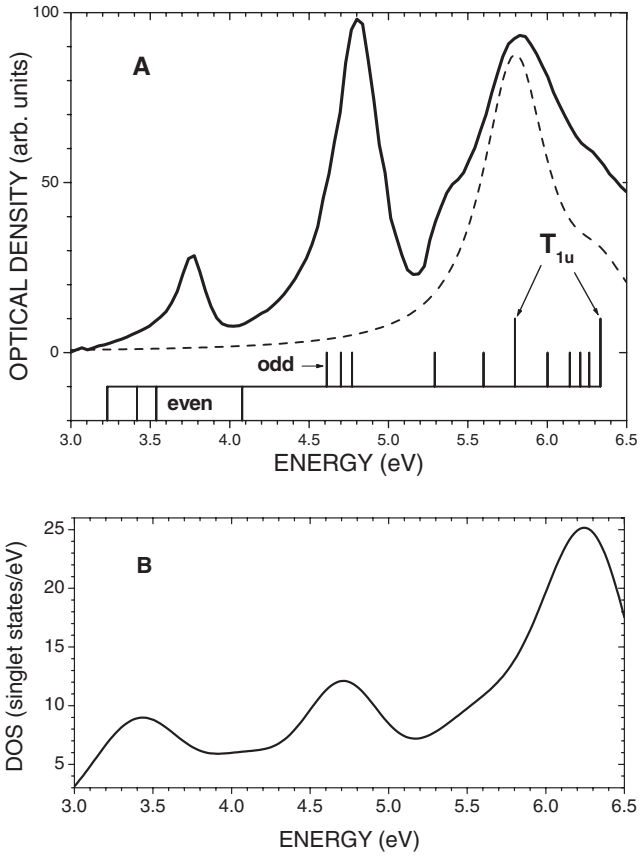

FIG. 1. Upper panel: Experimental optical density, Ref. [12], and the calculated spin singlet lines of C_{60}. The dashed line is the electronic contribution from two T_{1u} transitions broadened with linewidth of 0.5 eV. Lower panel: Density of singlet lines (broadened with linewidth of 0.5 eV).

The optical spectrum of C_{60} also shows some similarities with that of benzene [29,30]. The lowest excited states of benzene are spin triplets, while the first electronically allowed optical transition ($1\ ^1E_{1u}\leftarrow{}^1A_{1g}$) is situated at the relatively high energy of ~7 eV [30,31]. In benzene, the two lowest absorption bands at 4.90 and 6.20 eV were unambiguously assigned to the excited states of $1\ ^1B_{2u}$ and $1\ ^1B_{1u}$, respectively [30,31]. These bands are electronically forbidden and occur only due to the electron-vibronic coupling, which underlines the importance of the Herzberg-Teller mechanism [29] for the molecule. It is plausible that the same scenario applies to the C_{60} fullerene, and optical lines at smaller energies are caused by vibronic coupling to numerous electron states in these energy regions (Fig. 1). In Ref. [32]. the authors argue that the electron-vibronic interaction is very important for correct assignment of the absorption bands of C_{60}. It is worth noting that singlet and triplet states of C_{60} can be distinguished by low-energy electron spectroscopy [33].

Unfortunately, the electronic spectrum of C_{60} is not so well understood as benzene's, which has a long history of calculations and interpretations [29,30]. Although in all our SCI and SDCI calculations the $1\ ^1T_{1u}$ level remains at a high energy of ~6 eV, we think that there is still a possibility for it to be lowered if a calculation with a higher level of excitations within the CI approach is performed (at least SDTCI). Interestingly, this is the case for the first allowed optical transition ($1\ ^1E_{1u} \leftarrow {}^1A_{1g}$) in benzene. The CASSCF calculation of C_6H_6 (six π electrons distributed among 12 π MOs) places the $1\ ^1E_{1u}$ level at a high energy of 8.77 eV, while a multireference Møller-Plesset (MRMP) perturbation theory calculation on the CASSCF states lowers this energy by 1.84 eV to 6.93 eV (Table II of Ref. [30]). The last value is in perfect agreement with the experiment (6.94 eV, Ref. [31]). Notice that MRMP theory is known for effectively accounting for high excitations.

In conclusion, our SCI and SDCI calculations indicate that the first electronically allowed transition $1\ ^1T_{1u} \leftarrow {}^1A_{1g}$ is located at a relatively high energy of 5.8–6.0 eV. Our finding opens up a very interesting question on the assignment of the two lowest absorption bands at 3.8 and 4.8 eV found experimentally [12,13]. There are two ways to reconcile our calculations with the experiment. First, the $1\ ^1T_{1u}$ excited state can be lowered at the level of SDTCI or more refined CI calculations. The second scenario is the electron-vibronic coupling (Herzberg-Teller mechanism) [29], which is the case for benzene. Further investigations and *ab initio* calculations are needed to clarify this issue.

ACKNOWLEDGMENTS

We wish to thank one of the referees for many valuable remarks and for the suggestion of plotting Fig. 1(b). We are also grateful to Professor S. I. Strakhova from Moscow State University for providing us with helpful information.

[1] H. W. Kroto, J. R. Heath, S. C. O'Brien, R. F. Curl, and R. E. Smalley, Nature (London) **318**, 162 (1985).
[2] M. S. Dresselhaus, J. Dresselhaus, and P. C. Eklund, *Science of Fullerenes and Carbon Nanotubes* (Academic, New York, 1995).
[3] B. N. Plakhutin and R. Carbó-Dorca, Phys. Lett. A **267**, 370 (2000).
[4] E. Lo and B. R. Judd, Phys. Rev. Lett. **82**, 3224 (1999); B. R. Judd and E. Lo, J. Chem. Phys. **111**, 5706 (1999).
[5] A. V. Nikolaev and K. H. Michel, J. Chem. Phys. **117**, 4761 (2002).
[6] M. Wierzbowska, M. Lüders, and E. Tosatti, and J. Phys B **37**, 2685 (2004).
[7] S. Larsson, A. Volosov, and A. Rosén, Chem. Phys. Lett. **137**, 501 (1987).
[8] F. Negri, G. Orlandi, and F. Zerbetto, Chem. Phys. Lett. **144**, 31 (1988).
[9] I. László and L. Udvardi, J. Mol. Struct. THEOCHEM **183**, 271 (1989); I. László and L. Udvardi, Chem. Phys. Lett. **136**, 418 (1987).
[10] M. Braga, S. Larsson, A. Rosen, and A. Volosov, Astron. Astrophys. **245**, 232 (1991); M. Braga, A. Rosen, and S. Larsson, Z. Phys. D: At., Mol. Clusters **19**, 435 (1991).
[11] E. Westin, A. Rosén, G. Te Velde, and E. J. Baerends, J. Phys. B **29**, 5087 (1996).
[12] S. Leach, M. Vervloet, A. Desprès, E. Bréhert, J. P. Hare, T. J. Dennis, H. W. Kroto, R. Taylor, and D. R. M. Walton, Chem. Phys. **160**, 451 (1992).
[13] Z. Gasyna, P. N. Schatz, J. P. Hare, T. J. Dennis, H. W. Kroto, R. Taylor, and D. R. M. Walton, Chem. Phys. Lett. **183**, 283 (1991).
[14] C. C. Chancey and M. C. M. O'Brien, *The Jahn-Teller Effect in C_{60} and Other Icosahedral Complexes* (Princeton University Press, Princeton, NJ, 1997).
[15] K. Tanigaki and K. Prassides, J. Mater. Chem. **5**, 1515 (1995).
[16] L. Forró and L. Mihály, Rep. Prog. Phys. **64**, 649 (2001).
[17] A. Szabo and N. S. Ostlund, *Modern Quantum Chemistry* (Dover, New York, 1996).
[18] B. O. Roos and P. R. Taylor, Chem. Phys. **48**, 157 (1980); B. O. Roos, in *Advances in Chemical Physics: Ab Initio Methods in Quantum Chemistry—II*, Vol. 69, edited by K. P. Lawley (Wiley and Sons, Chichester, 1987), p. 399.
[19] J. C. Greer, Chem. Phys. Lett. **326**, 567 (2000).
[20] R. D. Johnson, G. Meijer, J. R. Salem, and D. S. Bethune, J. Am. Chem. Soc. **113**, 3619 (1991); W. I. F. David, R. M. Ibberson, J. C. Matthewman, K. Prassides, T. J. S. Dennis, J. P. Hare, H. W. Kroto, R. Taylor, and D. R. M. Walton, Nature (London) **353**, 147 (1991); A. K. Soper, W. I. F. David, D. S. Sivia, T. J. S. Dennis, J. P. Hare, and K. Prassides, J. Phys.: Condens. Matter **4**, 6087 (1992).
[21] The RHF code is a part of our original ALGOQMT package, which includes also the ALGOCI program. Examples of some calculations with the ALGORHF code are given in A. Artemyev, A. Bibikov, V. Zayets, and I. Bodrenko, J. Chem. Phys. **123**, 024103 (2005).
[22] O. Vahtras, J. Almlöf, and M. F. Feyereisen, Chem. Phys. Lett. **213**, 514 (1993).
[23] M. M. Francl, W. J. Pietro, W. J. Hehre, J. S. Binkley, M. S. Gordon, D. J. DeFrees, and J. A. Pople, J. Chem. Phys. **77**, 3654 (1982).
[24] Basis sets were obtained from the Extensible Computational Chemistry Environment Basis Set Database, Version 02/02/06 (EMSL), http://www.emsl.pnl.gov/forms/basisform.html
[25] T. H. Dunning, Jr., J. Chem. Phys. **90**, 1007 (1989).
[26] A. V. Nikolaev and I. Bodrenko, Algodign internal report, 2006 (unpublished).
[27] R. Rabilizirov, Astrophys. Space Sci. **125**, 331 (1986).
[28] F. Negri, G. Orlandi, and F. Zerbetto, J. Am. Chem. Soc. **114**, 2909 (1992).
[29] G. Herzberg, *Molecular Spectra and Molecular Structure* (Van Nostrand, Princeton, NJ, 1966), Vol. 3.
[30] T. Hashimoto, H. Nakano, and K. Hirao, J. Mol. Struct. THEOCHEM **451**, 25 (1998).
[31] A. Hiraya and K. Shobatake, J. Chem. Phys. **94**, 7700 (1991).
[32] F. Negri, G. Orlandi, and F. Zerbetto, J. Chem. Phys. **97**, 6496 (1992).
[33] J. P. Doering, J. Chem. Phys. **51**, 2866 (1969).